2024 IEEE 63rd Conference on Decision and Control (CDC)
December 16-19, 2024. MiCo, Milan, Italy

Encirclement Control for PDE-Based Leader-Follower Multi-Agent Systems with Targets in a Sphere: Part 2 – Rotation Encirclement

Milad Hasanzadeh[1] and Shu-Xia Tang[1]

2024 IEEE 63rd Conference on Decision and Control (CDC) | 979-8-3503-1633-9/24/$31.00 ©2024 IEEE | DOI: 10.1109/CDC56724.2024.10886038

***Abstract*— This paper introduces an innovative rotating encirclement control designed for parabolic Partial Differential Equation (PDE)-based multi-agent systems. The derivation of the PDE-based continuum multi-agent system model stems from techniques in flow system theory. The control strategy involves multi-step control within the domain and boundaries consisting of 2 parts. Initially in part 1, a successful target-enclosing control was applied to the system. After successfully achieving enclosing, here in part 2 of the paper, the agents face further challenges, including rotating around targets and adjusting their formation to maintain the encirclement. To address these challenges, in-domain control is applied to the agents, ensuring compliance with all requirements. Employing successive multi-step controls in a distributed manner is crucial for improving tracking and coordination among the agents, thus enhancing the effectiveness of the encirclement control. Stability analysis of the closed-loop system is conducted using the Lyapunov technique. Finally, simulations are conducted to evaluate the effectiveness of our proposed methodology. It is worth mentioning that part 2 stands as an independent outcome, tackling the challenge of rotating encirclement by leveraging a target-enclosing formation.**

***Index Terms*— Multi-Agent Systems, Encirclement Control, PDE control, In-domain control, Finite difference method.**

I. Introduction

Advancements in modeling large-scale multi-agent systems (MASs) have shifted towards a continuum-based approach, primarily utilizing PDE models as pioneered by [1]–[3]. Building upon this framework, [4] introduced partial difference equations (PdEs) over graphs to analyze collective dynamics, serving as the basis for employing PDEs in modeling multi-agent systems. Specifically, finite-difference approximations map space variables to agent indices and transform spatial derivatives into links between neighbors [5], [6], enabling the formulation of collective dynamics as a PDE for large groups of discrete agents.

[7] presents two approaches that involve collaboration between climbing and ground robots to tackle the mapping challenge for autonomous inspection of three-dimensional (3D) structures. [8] studied how to plan the movement of multi-agent systems using flatness-based method that helps them form specific shapes on a plane within a set time, following paths that are already planned. [9] recently investigated the deployment of agents distributed on a disk-shaped grid onto three-dimensional profiles using backstepping approach. In [10], formation control of MASs is investigated using two 2-D reaction-advection-diffusion PDEs to model the system's dynamics. These PDEs represent the positions of agents, where the first one is complex-valued. The second PDE is real-valued and describes height.

Encirclement is a significant application of MAS, where a collective of agents collaborates to enclose a target entity, which could be either a moving intruder or a stationary object, see [11]. This control strategy has attracted significant interest across different domains such as search and rescue missions [12], and object tracking [13]. Encirclement control which we are aiming for here, operates on the premise that a specific number of targets are present, and the objective of the agents is to encircle these targets and orbit around them, as in [14].

In our previous research, we investigated encirclement control for MAS modeled by Ordinary Differential Equations (ODEs). Specifically, [14] explored distributed dynamic encirclement control for first-Order multi-Agent systems in the presence of communication delay. Additionally, [11] focused on distributed fixed-time rotating encirclement control of linear multi-agent systems with moving targets. In our current study, we utilize the model presented in our previous work on formation control [10], and the encirclement control algorithm enables agents to autonomously navigate towards target locations and surround them. Upon successful encirclement, the agents execute rotational movements around the targets.

- To the best of the author's knowledge, this study presents the first introduction of rotational encirclement control specifically designed for PDE-based multi-agent systems. The emphasis lies on multi-step control strategies applied within both the domain and boundaries.
- Compared with [10] which focus on the PDE-based multi-agent formation control, this paper introduces several advancements. One notable contribution lies in PDE-based **encirclement control** where both boundary control and **in-domain** control design has been used to form encirclement and a multi-step control design has been applied.
- Compared with works in [14] which focus on the encirclement control for ODE-based models on 2D surface, this paper differentiate itself by **PDE-based model** for multi-agent systems on 3D coordinate where **large-scale MAS** is considered here.

II. Problem Statement

Encirclement control involves designing a controller for $n \times m$ agents to surround p targets, ensuring agents encircle and rotate around the targets without collisions as shown

[1]Milad Hasanzadeh and Shu-Xia Tang (corresponding author) are with the Department of Mechanical Engineering, Texas Tech University, Texas, USA m.hasanzadeh@ttu.edu, shuxia.tang@ttu.edu.

Authorized licensed use limited to: Texas Tech University. Downloaded on March 19,2025 at 18:54:39 UTC from IEEE Xplore. Restrictions apply.

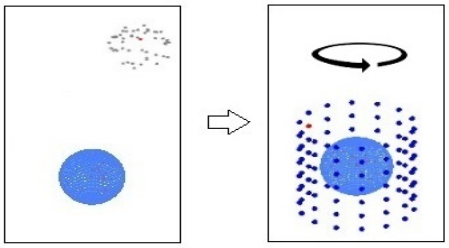

Fig. 1: Gray spheres represent agents in their initial positions, while blue spheres represent their intended positions during encirclement. Additionally, the larger cyan sphere indicates the space occupied by the targets.

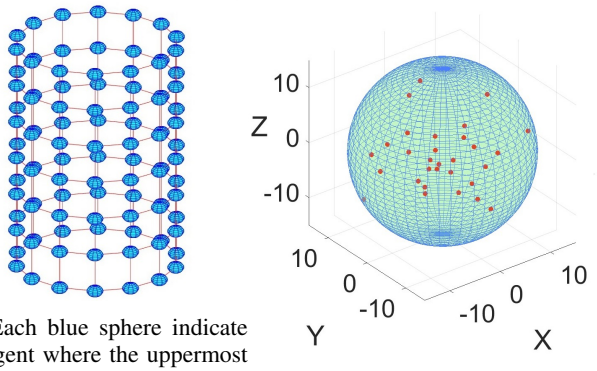

(a) Each blue sphere indicate an agent where the uppermost and lowermost layers consist of leaders.

(b) Targets are pointed with red spheres inside the light green sphere.

Fig. 2

in Fig. 1. To prevent collisions, we use a PDE system with specific boundary conditions, assigning unique IDs to agents to maintain distinct positions in cylindrical space. To prevent collision among agents with targets, the encirclement process is divided into four steps, each addressing a specific challenge. Once the control in the current step addressed the challenge, the subsequent control was applied to address the next challenge accordingly. Let $\Xi = \{1, 2, 3, 4\}$ represent the set of all steps. Steps one to three were addressed in the concept of boundary control in first part of paper in [15] and the last step will be treated as in-domain control here. In this section, we provide the profile of the group of p targets represented by $\Phi = \{1, 2, ..., p\}$, the model representing the dynamics of $n \times m$ agents denoted as $\Psi = \{(i, j) : \forall i \in \{1, ..., n\}, \forall j \in \{1, ..., m\}\}$, and the review of target-enclosing problem defined and addressed in part 1 of paper and the encirclement problem definition.

A. Targets' Profile

Throughout the paper, the position of target $i \in \Phi$ in 3D space along the coordinate axes (x, y, z) is denoted as $\boldsymbol{w}_i^{\text{ta}}(t) = [x_i^{\text{ta}}(t), y_i^{\text{ta}}(t), z_i^{\text{ta}}(t)]^T$. For simplicity, in the remainder of this paper, we abbreviate $\boldsymbol{w}_i^{\text{ta}}(t)$ as $\boldsymbol{w}_i^{\text{ta}}$. The dynamics of targets are governed by the following assumptions.

Assumption 1: $\boldsymbol{w}_i^{\text{ta}}$, $\forall i \in \Phi$, are continuously differentiable and the velocity of targets $\forall t > 0$ is bounded as

$$\|\dot{\boldsymbol{w}}_i^{\text{ta}}\| \leqslant \beta, \tag{1}$$

where β is a positive constant.

Assumption 2: Targets will not collide with each other, that is $\forall t > 0, i, j, i \neq j \in \Phi$,

$$\boldsymbol{w}_j^{\text{ta}} \neq \boldsymbol{w}_i^{\text{ta}}. \tag{2}$$

Assumption 3: Targets' dynamics are bounded that means the movements of targets are limited within a spherical area that is $\forall i \in \Phi$ we have

$$\sup_{t>0} \|\boldsymbol{w}_i^{\text{ta}}(t) - \boldsymbol{w}^{\star}\| \leqslant r^{\star}, \tag{3}$$

where $\boldsymbol{w}^{\star} = [x^{\star}, y^{\star}, z^{\star}]^T, r^{\star}$ are the center and the radius of the sphere.

Figure 2b is demonstrating the location of targets in the spherical area described by Assumption 3.

B. Agents' Dynamic

A group of $n \times m$ agents navigating in a 3D space along the coordinate axes (x, y, z). n stands for the total number of agents (blue spheres) in each circle of the cylindrical mesh grid shown in Fig. (2a) and m stands for the total number of circles of the cylindrical mesh grid. To streamline the notation, we introduce the complex-valued variable $u = x + jy$ to represent the state components on the (x, y) axes. An indirect topology graph is defined on a cylindrical surface, as shown in Figure 2a, to determine the neighbor set of each agent. As the number of agents increases, particularly for large m and n, we consider the agents as a continuum, enabling the mapping of discrete identification (ID) numbers (i, j) of the agents (θ_i, s_j) to coordinates on the cylindrical surface $\Omega = \{(\theta, s) : -\pi \leqslant \theta < \pi, 0 \leqslant s \leqslant 1\}$. This mapping, $(\theta_i, s_j) \to (\theta, s)$, occurs as $m, n \to \infty$. Consequently, the multi-agent systems, operating on a large scale, are effectively modeled as PDE. In this section, we aim to use linear parabolic PDE to describe the collective dynamics of the multi-agent system. Consider the position of agent $(i, j) \in \Psi$ in 3D space is denoted as $u^{\text{ag}}(t, \theta, s)$ along with $z^{\text{ag}}(t, \theta, s)$. Based on the concept of boundary actuation, leaders are selected from agents positioned at the uppermost and lowermost layers of the topology surface shown in Figure 2a. The collective dynamics of the agent system is modeled by a system of two reaction–advection–diffusion PDE as

$$\begin{aligned} u_t^{\text{ag}}(t, \theta, s) =& \Delta u^{\text{ag}}(t, \theta, s) + \alpha_1 u_s^{\text{ag}}(t, \theta, s) + \zeta_1 u^{\text{ag}}(t, \theta, s) \\ &+ U(t, \theta), \end{aligned} \tag{4a}$$

$$\begin{aligned} z_t^{\text{ag}}(t, \theta, s) =& \Delta z^{\text{ag}}(t, \theta, s) + \alpha_2 z_s^{\text{ag}}(t, \theta, s) + \zeta_2 z^{\text{ag}}(t, \theta, s) \\ &+ Z(t, \theta), \end{aligned} \tag{4b}$$

$$u^{\text{ag}}(t, \theta, 0) = f_1(\theta), \quad u^{\text{ag}}(t, \theta, 1) = g_1(\theta), \tag{4c}$$

$$u^{\text{ag}}(t, -\pi, s) = u^{\text{ag}}(t, \pi, s) \tag{4d}$$

$$z^{\text{ag}}(t, \theta, 0) = f_2(\theta), \quad z^{\text{ag}}(t, \theta, 1) = g_2(\theta), \tag{4e}$$

$$z^{\text{ag}}(t, -\pi, s) = z^{\text{ag}}(t, \pi, s). \tag{4f}$$

In the context of $(t, \theta, s) \in \mathbb{R}^+ \times \Omega$, where θ and s represent spatial variables and agent IDs on the communication topology, respectively, $u, \alpha_1, \zeta_1 \in \mathbb{C}$ and $z, \alpha_2, \zeta_2 \in \mathbb{R}$. Ad-

Authorized licensed use limited to: Texas Tech University. Downloaded on March 19,2025 at 18:54:39 UTC from IEEE Xplore. Restrictions apply.

ditionally, $f_1(\theta), g_1(\theta)$ and $f_2(\theta), g_2(\theta)$ denote non-zero and bounded boundary conditions for states u and z, respectively, representing the open-loop formation of leaders. Controllers $U(t,\theta)$ and $Z(t,\theta)$ will be designed for horizontal and vertical coordinates to stabilize the system to certain desired profile. The system modeled in (4) is utilized for the last challenge in the problem. Δ denotes the Laplace operator as

$$\Delta u^{\mathrm{ag}}(t,\theta,s) = u^{\mathrm{ag}}_{\theta\theta}(t,\theta,s) + u^{\mathrm{ag}}_{ss}(t,\theta,s),$$
$$\Delta z^{\mathrm{ag}}(t,\theta,s) = z^{\mathrm{ag}}_{\theta\theta}(t,\theta,s) + z^{\mathrm{ag}}_{ss}(t,\theta,s).$$

The explicit solution of the complex-valued state in part 1 was

$$\bar{u}^{\mathrm{ag}}(\theta,s) = \begin{cases} \sum_{k=-\infty}^{\infty} \mathrm{e}^{\mathrm{j}k\theta - \frac{1}{2}\alpha_1 s}\left(A_k \mathrm{e}^{\sqrt{a}s} + B_k \mathrm{e}^{-\sqrt{a}s}\right), \\ \qquad \text{if} \quad a > 0, \\ \sum_{k=-\infty}^{\infty} \mathrm{e}^{\mathrm{j}k\theta}\left(A_k \mathrm{e}^{-\frac{1}{2}\alpha_1 s} + B_k s \mathrm{e}^{-\frac{1}{2}\alpha_1 s}\right), \\ \qquad \text{if} \quad a = 0, \\ \sum_{k=-\infty}^{\infty} \mathrm{e}^{\mathrm{j}k\theta - \frac{1}{2}\alpha_1 s}\left(A_k \cos\left(\frac{1}{2}\sqrt{-a}s\right)\right. \\ \left. + B_k \sin\left(\frac{1}{2}\sqrt{-a}s\right)\right), \\ \qquad \text{if} \quad a < 0. \end{cases} \tag{5}$$

In this section, the objective for the agents is to execute a series of actions, including rotating around targets, and if required, adjusting their formation to sustain the encirclement. Rotation cause time-varing solution in the desired profile and for this reason the solution in (5) changes into following

$$\bar{u}^{\mathrm{ag}}(t,\theta,s) = \begin{cases} \sum_{k=-\infty}^{\infty} \mathrm{e}^{\mathrm{j}(t+k\theta) - \frac{1}{2}\alpha_1 s}\left(A_k \mathrm{e}^{\sqrt{a}s} + B_k \mathrm{e}^{-\sqrt{a}s}\right), \\ \qquad \text{if} \quad a > 0, \\ \sum_{k=-\infty}^{\infty} \mathrm{e}^{\mathrm{j}(t+k\theta)}\left(A_k \mathrm{e}^{-\frac{1}{2}\alpha_1 s} + B_k s \mathrm{e}^{-\frac{1}{2}\alpha_1 s}\right), \\ \qquad \text{if} \quad a = 0, \\ \sum_{k=-\infty}^{\infty} \mathrm{e}^{\mathrm{j}(t+k\theta) - \frac{1}{2}\alpha_1 s}\left(A_k \cos\left(\frac{1}{2}\sqrt{-a}s\right)\right. \\ \left. + B_k \sin\left(\frac{1}{2}\sqrt{-a}s\right)\right), \\ \qquad \text{if} \quad a < 0, \end{cases} \tag{6}$$

where A_k and B_k are constants determined by the boundary conditions given in equations. Since rotation does not happen along z axis then $\bar{z}^{\mathrm{ag}}(\theta,s)$ stays without changes as a time invariant function.

The desired geometric center of the system at each step was defined as $(u_i^{\diamond}, z_i^{\diamond}), \forall i \in \Xi$ where we could define the desired profile of agents $\forall i \in \Xi$ as

$$\tilde{u}_i^{\mathrm{ag}}(t,\theta,s) = u_i^{\diamond} + \bar{u}_i^{\mathrm{ag}}(t,\theta,s), \tilde{z}_i^{\mathrm{ag}}(t,\theta,s) = z_i^{\diamond} + \bar{z}_i^{\mathrm{ag}}(t,\theta,s). \tag{7}$$

The objective in each step was to design $U(t,\theta)$ and $Z(t,\theta)$ such that $(u^{\mathrm{ag}}(t,\theta,s), z^{\mathrm{ag}}(t,\theta,s)) \to (\tilde{u}_i^{\mathrm{ag}}(\theta,s), \tilde{z}_i^{\mathrm{ag}}(\theta,s))$. Consequently, the controllers were denoted as $U_i(t,\theta)$ and $Z_i(t,\theta)$. The error signals were be defined as

$$u_i^{\mathrm{er}}(t,\theta,s) = u^{\mathrm{ag}}(t,\theta,s) - \tilde{u}_i^{\mathrm{ag}}(\theta,s), \tag{8}$$
$$z_i^{\mathrm{er}}(t,\theta,s) = z^{\mathrm{ag}}(t,\theta,s) - \tilde{z}_i^{\mathrm{ag}}(\theta,s), \tag{9}$$

then the error dynamics for the system modeled by (4) are

$$\begin{aligned} u^{\mathrm{er}}_{i_t}(t,\theta,s) &= \Delta u_i^{\mathrm{er}}(t,\theta,s) + \alpha_1 u^{\mathrm{er}}_{i_s}(t,\theta,s) + \zeta_1 u_i^{\mathrm{er}}(t,\theta,s) \\ &\quad + \Delta \tilde{u}_i^{\mathrm{ag}}(\theta,s) + \alpha_1 \tilde{u}^{\mathrm{ag}}_{i_s}(\theta,s) + \zeta_1 \tilde{u}_i^{\mathrm{ag}}(\theta,s) \\ &\quad - \tilde{u}^{\mathrm{ag}}_{i_t}(\theta,s) + U_i(t,\theta), \end{aligned} \tag{10a}$$
$$\begin{aligned} z^{\mathrm{er}}_{i_t}(t,\theta,s) &= \Delta z_i^{\mathrm{er}}(t,\theta,s) + \alpha_2 z^{\mathrm{er}}_{i_s}(t,\theta,s) + \zeta_2 z_i^{\mathrm{er}}(t,\theta,s) \\ &\quad + \Delta \tilde{z}_i^{\mathrm{ag}}(\theta,s) + \alpha_2 \tilde{z}^{\mathrm{ag}}_{i_s}(\theta,s) + \zeta_2 \tilde{z}_i^{\mathrm{ag}}(\theta,s) \\ &\quad - \tilde{z}^{\mathrm{ag}}_{i_t}(\theta,s) + Z_i(t,\theta), \end{aligned} \tag{10b}$$
$$u_i^{\mathrm{er}}(t,\theta,0) = 0, \quad u_i^{\mathrm{er}}(t,\theta,1) = 0, \tag{10c}$$
$$u_i^{\mathrm{er}}(t,0,s) = u_i^{\mathrm{er}}(t,2\pi,s) \tag{10d}$$
$$z_i^{\mathrm{er}}(t,\theta,0) = 0, \quad z_i^{\mathrm{er}}(t,\theta,1) = 0, \tag{10e}$$
$$z_i^{\mathrm{er}}(t,0,s) = z_i^{\mathrm{er}}(t,2\pi,s). \tag{10f}$$

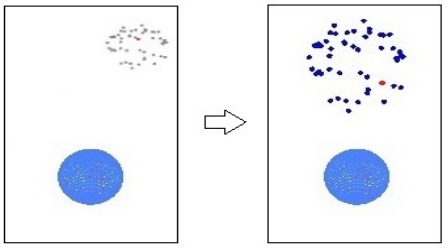

Fig. 3: Translation of agents. Gray spheres represent agents in their initial positions, while blue spheres represent their intended positions at this step.

C. Target-Enclosing Review

In each step, we will define a steady-state solution for the required formation and desired geometric center, establishing a unique profile as in (7). The error dynamics will be adapted to this profile. Steps 1 to 3 focus on stabilizing error dynamics at boundaries and are addressed in [15], while step 4 targets stabilization in (10). We will also analyze the dynamics of $u_i^{\mathrm{er}}(t,\theta,s)$ and $z_i^{\mathrm{er}}(t,\theta,s)$ for each step.

1) Step 1: Translation: In step 1, the goal is to move agents to the upper side of the targets without following a specific formation. This involves setting the desired geometric center based on the upper side of the targets and using a steady-state solution of zero. Figure 3 shows this step. Boundary agents act as leaders using backstepping to stabilize error dynamics, while other agents follow them to avoid collisions. The objective for step 1 is

$$\begin{aligned} &\|u^{\mathrm{ag}}(t,\cdot) - u^{\star}\|_{L^2} \leqslant \nu_1 e^{-\frac{1}{2}t}\|u^{\mathrm{ag}}(0,\cdot) - u^{\star}\|_{L^2}, \\ &\|z^{\mathrm{ag}}(t,\cdot) - \xi z^{\star}\|_{L^2} \leqslant \nu_2 e^{-\frac{1}{2}t}\|z^{\mathrm{ag}}(0,\cdot) - \xi z^{\star}\|_{L^2}, \end{aligned} \tag{11}$$

where $u^{\star} = x^{\star} + jy^{\star}$, $x^{\star}, y^{\star}$, and $z^{\star}$ are the center of the target sphere, $\xi > 1$ is a design parameter, and ν_1 and ν_2 are positive constants.

Authorized licensed use limited to: Texas Tech University. Downloaded on March 19,2025 at 18:54:39 UTC from IEEE Xplore. Restrictions apply.

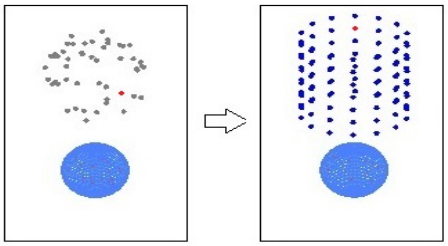

Fig. 4: Formation of agents. Gray spheres represent agents in their initial positions, while blue spheres represent their intended positions at this step.

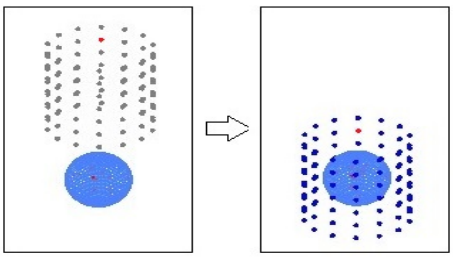

Fig. 5: Target-enclosing by agents. Gray spheres represent agents in their initial positions, while blue spheres represent their intended positions at this step. Additionally, the larger cyan sphere indicates the space occupied by the targets.

2) Step 2: Formation: In step 2, the goal is to form a cylindrical shape above the targets, avoiding collisions. The cylinder's radius will be larger than the target sphere's, and agents' positions will be maintained. We start with a steady-state solution for the cylindrical formation, setting the desired geometric center to zero. As in step 1, boundary agents lead, guiding the formation while others follow. Figure 4 illustrates this step. The objective is

$$\begin{aligned}\|u^{\mathrm{ag}}(t,\cdot)-\bar{u}(\cdot)\|_{L^2}&\leqslant \nu_3 e^{-\frac{1}{2}t}\|u^{\mathrm{ag}}(0,\cdot)-\bar{u}(\cdot)\|_{L^2},\\ \|z^{\mathrm{ag}}(t,\cdot)-\bar{z}(\cdot)\|_{L^2}&\leqslant \nu_4 e^{-\frac{1}{2}t}\|z^{\mathrm{ag}}(0,\cdot)-\bar{z}(\cdot)\|_{L^2},\end{aligned} \tag{12}$$

where ν_3 and ν_4 are positive constants.

3) Step 3: Enclosing: In step 3, the goal is to move agents downward to enclose all target spheres within the cylindrical formation, avoiding collisions since the cylinder's radius exceeds that of the spheres. The desired geometric center of the agents will align with the center of the target spheres, with the steady-state solution set to zero to maintain the formation. Figure 5 shows this step. Boundary agents lead, while others follow, with the challenge being distributed relocation. The objective for step 3 is

$$\begin{aligned}\|u^{\mathrm{ag}}(t,\cdot)-u^{\star}\|_{L^2}&\leqslant \nu_5 e^{-\frac{1}{2}t}\|u^{\mathrm{ag}}(0,\cdot)-u^{\star}\|_{L^2},\\ \|z^{\mathrm{ag}}(t,\cdot)-z^{\star}\|_{L^2}&\leqslant \nu_6 e^{-\frac{1}{2}t}\|z^{\mathrm{ag}}(0,\cdot)-z^{\star}\|_{L^2},\end{aligned} \tag{13}$$

where ν_5 and ν_6 are positive constants.

Theorem 1: Consider the system described by equations (14), where the controller is activated at the boundaries

$$u_t^{\mathrm{ag}}(t,\theta,s)=\Delta u^{\mathrm{ag}}(t,\theta,s)+\alpha_1 u_s^{\mathrm{ag}}(t,\theta,s)+\zeta_1 u^{\mathrm{ag}}(t,\theta,s), \tag{14a}$$

$$u^{\mathrm{ag}}(t,\theta,0)=f_1(\theta),\quad u^{\mathrm{ag}}(t,\theta,1)=g_1(\theta)+U_i(t,\theta), \tag{14b}$$

$$u^{\mathrm{ag}}(t,-\pi,s)=u^{\mathrm{ag}}(t,\pi,s). \tag{14c}$$

In the initial phase of the study [15], 3 separate control steps applied and we designed the controllers $U_i(t,\theta),\forall i\in\{1,2,3\}$ as follows

$$\begin{aligned}U_1(t,\theta)=&-\int_0^1 \lambda_1\tau\frac{\mathrm{I}_1\left[\sqrt{\lambda_1(1-\tau^2)}\right]}{\sqrt{\lambda_1(1-\tau^2)}}\mathrm{e}^{-\frac{1}{2}\alpha_1(1-\tau)}\\ &\times(u^{\mathrm{ag}}(t,\theta,\tau)-\tilde{u}_1^{\mathrm{ag}}(\theta,\tau))d\tau,\end{aligned} \tag{15}$$

$$\begin{aligned}U_2(t,\theta)=&-\int_0^1 \lambda_1\tau\frac{\mathrm{I}_1\left[\sqrt{\lambda_1(1-\tau^2)}\right]}{\sqrt{\lambda_1(1-\tau^2)}}\mathrm{e}^{-\frac{1}{2}\alpha_1(1-\tau)}\\ &\times(u^{\mathrm{ag}}(t,\theta,\tau)-\tilde{u}_2^{\mathrm{ag}}(\theta,\tau))d\tau,\end{aligned} \tag{16}$$

and

$$\begin{aligned}U_3(t,\theta)=&-\int_0^1 \lambda_1\tau\frac{\mathrm{I}_1\left[\sqrt{\lambda_1(1-\tau^2)}\right]}{\sqrt{\lambda_1(1-\tau^2)}}\mathrm{e}^{-\frac{1}{2}\alpha_1(1-\tau)}\\ &\times(u^{\mathrm{ag}}(t,\theta,\tau)-\tilde{u}_3^{\mathrm{ag}}(\theta,\tau))d\tau,\end{aligned} \tag{17}$$

where $\lambda_1=\zeta_1-\frac{1}{4}\alpha_1^2$ and I_1 is the first-order modified Bessel function of the first-kind. $\tilde{u}_i^{\mathrm{ag}}(\theta,\tau)$ is the desired profile at step i defined in (7) where based on (7) and Table I one could obtain the desired profile for each step separately. By sequentially activating controllers $U_i(t,\theta),\forall i\in\{1,2,3\}$ in the system (14), the system state exponentially converged to the desired profiles, as expressed by:

$$\|u^{\mathrm{ag}}(t,\cdot)-\tilde{u}_i^{\mathrm{ag}}(\cdot)\|_{L^2}\leqslant \nu_i e^{-\frac{1}{2}t}\|u^{\mathrm{ag}}(0,\cdot)-\tilde{u}_i^{\mathrm{ag}}(\cdot)\|_{L^2}, \tag{18}$$

where ν_i are positive constants, leading to the successful target-enclosing.

Steps	Geometric center	Formation
translation	$x^\star+jy^\star$,$\xi z^\star$	-
formation	-	$f_1=g_1=kr^\star e^{j\theta}, f_2=0, g_2=1$
enclosing	$x^\star+jy^\star$,$z^\star$	-
Rotation	-	$f_1=g_1=kr^\star e^{j(t+\theta)}, f_2=-10, g_2=10$

TABLE I: Desired profile

Subsequent sections will concentrate on devising stabilization control designs for the $u_i^{\mathrm{er}}(t,\theta,s)$ system outlined in (10) for step 4 in detail.

D. Rotating Encirclement

In step 4, the goal is for agents to rotate around the target sphere and adjust their formation without collisions. We use a time-varying solution for rotation instead of a steady-state one, with the desired geometric center set to zero to prevent movement. Unlike previous steps with boundary leaders,

Authorized licensed use limited to: Texas Tech University. Downloaded on March 19,2025 at 18:54:39 UTC from IEEE Xplore. Restrictions apply.

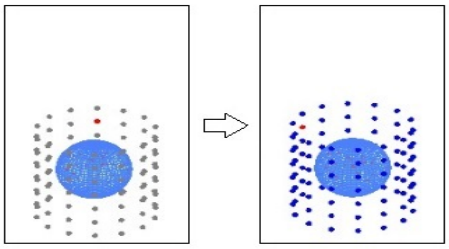

Fig. 6: Rotating encirclement of targets by agents. Gray spheres represent agents in their initial positions, while blue spheres represent their intended positions at this step. The agent colored in red indicate rotation at the intended position.

this step uses in-domain control, allowing agents to lead themselves. The challenge is dynamic, distributed tracking of the time-varying profile. Figure 6 shows this step. The objective for step 4 is

$$\begin{aligned}\|u^{\mathrm{ag}}(t,\cdot)-\bar{u}(t,\cdot)\|_{L^2}&\leqslant \nu_7 e^{-\frac{1}{2}t}\|u^{\mathrm{ag}}(0,\cdot)-\bar{u}(0,\cdot)\|_{L^2},\\ \|z^{\mathrm{ag}}(t,\cdot)-\bar{z}(t,\cdot)\|_{L^2}&\leqslant \nu_8 e^{-\frac{1}{2}t}\|z^{\mathrm{ag}}(0,\cdot)-\bar{z}(0,\cdot)\|_{L^2},\end{aligned} \tag{19}$$

where ν_7 and ν_8 are positive constants. The challenge in this step is rotation and adjustment of agents' formation and it will be resolved accordingly in this part of paper.

III. Step 4: Rotation

This section aims to make agents rotate and adjust their formation around targets without collisions, as shown in Fig. 6. Substituting (6) into (7) yields the desired profile.

$$\tilde{u}_4^{\mathrm{ag}}(t,\theta,s)=\bar{u}_4^{\mathrm{ag}}(t,\theta,s),\tilde{z}_4^{\mathrm{ag}}(\theta,s)=\bar{z}_4^{\mathrm{ag}}(\theta,s). \tag{20}$$

By substituting (20) in the error dynamic (10) the representative error dynamic is as follow

$$\begin{aligned}u_{4_t}^{\mathrm{er}}(t,\theta,s)=&\Delta u_4^{\mathrm{er}}(t,\theta,s)+\alpha_1 u_{4_s}^{\mathrm{er}}(t,\theta,s)+\zeta_1 u_4^{\mathrm{er}}(t,\theta,s)\\&+\Delta\tilde{u}_4^{\mathrm{ag}}(t,\theta,s)+\alpha_1\tilde{u}_{4_s}^{\mathrm{ag}}(t,\theta,s)+\zeta_1\tilde{u}_4^{\mathrm{ag}}(t,\theta,s)\\&-\tilde{u}_{4_t}^{\mathrm{ag}}(t,\theta,s)+U_4(t,\theta,s),\end{aligned} \tag{21a}$$

$$\begin{aligned}z_{4_t}^{\mathrm{er}}(t,\theta,s)=&\Delta z_4^{\mathrm{er}}(t,\theta,s)+\alpha_2 z_{4_s}^{\mathrm{er}}(t,\theta,s)+\zeta_2 z_4^{\mathrm{er}}(t,\theta,s)\\&+\zeta_2\tilde{z}_4^{\mathrm{ag}}+Z_4(t,\theta,s),\end{aligned} \tag{21b}$$

$$u_4^{\mathrm{er}}(t,\theta,0)=0,\quad u_4^{\mathrm{er}}(t,\theta,1)=0, \tag{21c}$$

$$u_4^{\mathrm{er}}(t,0,s)=u_4^{\mathrm{er}}(t,2\pi,s). \tag{21d}$$

In order to stabilize the error dynamic we have used the Lyapunov based design to achieve the exponential stability in the sense of L_2 norm required actions by this step, the following input controls has been proposed.

$$\begin{aligned}U_4(t,\theta,s)=&-\alpha_1 u_{4_s}^{\mathrm{er}}(t,\theta,s)+\kappa_1 u_4^{\mathrm{er}}(t,\theta,s)\\&-\Delta\tilde{u}_4^{\mathrm{ag}}(t,\theta,s)-\alpha_1\tilde{u}_{4_s}^{\mathrm{ag}}(t,\theta,s)\\&-\zeta_1\tilde{u}_4^{\mathrm{ag}}(t,\theta,s)+\tilde{u}_{4_t}^{\mathrm{ag}}(t,\theta,s),\end{aligned} \tag{22}$$

$$Z_4(t,\theta,s)=-\alpha_2 z_{4_s}^{\mathrm{er}}(t,\theta,s)+\kappa_2 z_4^{\mathrm{er}}(t,\theta,s)-\zeta_2\tilde{z}_4^{\mathrm{ag}}, \tag{23}$$

where κ_1 and κ_2 are design parameters. After actuating $U_4(t,\theta,s)$ and $Z_4(t,\theta,s)$ into the error system in (21), the error dynamic are mapped to the followings

$$u_{4_t}^{\mathrm{er}}(t,\theta,s)=\Delta u_4^{\mathrm{er}}(t,\theta,s)+(\zeta_1+\kappa_1)u_4^{\mathrm{er}}(t,\theta,s), \tag{24a}$$

$$z_{4_t}^{\mathrm{er}}(t,\theta,s)=\Delta z_4^{\mathrm{er}}(t,\theta,s)+(\zeta_2+\kappa_2)z_4^{\mathrm{er}}(t,\theta,s), \tag{24b}$$

$$u_4^{\mathrm{er}}(t,\theta,0)=0,\quad u_4^{\mathrm{er}}(t,\theta,1)=0, \tag{24c}$$

$$u_4^{\mathrm{er}}(t,0,s)=u_4^{\mathrm{er}}(t,2\pi,s), \tag{24d}$$

Here, the terms for the desired profile and advection terms are removed. Additive reaction terms with coefficients κ_1 and κ_2 help converge the model's reaction terms to zero.

Theorem 2: Consider the error dynamic in (4) in conjunction with the control design described by (22). Consider the error signal definition in (8). The error system dynamic is exponentially stable in the sense of L_2 norm if $\kappa_1=\zeta_1-1$ and $\kappa_2=\zeta_2-1$ then we have

$$\|u_4^{\mathrm{er}}(t,\cdot)\|_{L^2}\leqslant\nu_7 e^{-\frac{1}{2}t}\|u_4^{\mathrm{er}}(0,\cdot)\|_{L^2},$$

where ν_7 is a positive constant. It is equivalent to

$$\|u^{\mathrm{ag}}(t,\cdot)-\tilde{u}_4^{\mathrm{ag}}(t,\cdot)\|_{L^2}\leqslant\nu_7 e^{-\frac{1}{2}t}\|u^{\mathrm{ag}}(0,\cdot)-\tilde{u}_4^{\mathrm{ag}}(0,\cdot)\|_{L^2}.$$

The system state is exponentially convergent to the desired profile in the sense of L_2 norm.

We select κ_1 and κ_2 based on ζ_1 and ζ_2 such that $\zeta_1+\kappa_1$ and $\zeta_2+\kappa_2$ are both negative. The proof is omitted due to page limitations.

For $\nu_8>0$, the behavior of $z^{\mathrm{ag}}(t,\theta,s)$ with control design (22) closely resembles the first system state, leading to the following conclusion.

$$\|z^{\mathrm{ag}}(t,\cdot)-\tilde{z}_4^{\mathrm{ag}}(\cdot)\|_{L^2}\leqslant\nu_8 e^{-\frac{1}{2}t}\|z^{\mathrm{ag}}(0,\cdot)-\tilde{z}_4^{\mathrm{ag}}(\cdot)\|_{L^2}.$$

IV. Simulation

A. Discretization of PDE system

To fully encircle the targets, we simulate the first part of the paper and use the final positions from step 3 as the initial condition for step 4. We apply the control design from (22) to the system using the central finite difference method to discretize the system in Ω space for $i=1,\cdots,n$, $j=1,\cdots,m$, and $k=1,\cdots,q$.

$$\theta_i=(i-1)\Delta\theta, s_j=(j-1)\Delta s, t_k=(k-1)\Delta t \tag{25}$$

$$\Delta\theta=\frac{2\pi}{n-1},\Delta s=\frac{1}{m-1},\Delta t=\frac{t_{\max}-t_{\min}}{q-1}, \tag{26}$$

where q is selected to be sufficiently large to ensure the time step Δt is adequately small. The subsequent formulas are applied to all points (agents).

$$\begin{aligned}u_{k+1,i,j}^{\mathrm{ag}}=&u_{k.i.j}^{\mathrm{ag}}+\frac{\Delta t}{\Delta\theta^2}(u_{k,i+1,j}^{\mathrm{ag}}-2u_{k,i,j}^{\mathrm{ag}}+u_{k,i-1,j}^{\mathrm{ag}})\\&+\frac{\Delta t}{\Delta s^2}(u_{k,i,j+1}^{\mathrm{ag}}-2u_{k,i,j}^{\mathrm{ag}}+u_{k,i,j-1}^{\mathrm{ag}})\\&+\alpha_1\frac{\Delta t}{2\Delta s}(u_{k,i,j+1}^{\mathrm{ag}}-u_{k,i,j-1}^{\mathrm{ag}})+\zeta_1 u_{k,i,j}^{\mathrm{ag}},\end{aligned} \tag{27}$$

$$\begin{aligned}z_{k+1,i,j}^{\mathrm{ag}}=&z_{k,i,j}^{\mathrm{ag}}+\frac{\Delta t}{\Delta\theta^2}(z_{k,i+1,j}^{\mathrm{ag}}-2z_{k,i,j}^{\mathrm{ag}}+z_{k,i-1,j}^{\mathrm{ag}})\\&+\frac{\Delta t}{\Delta s^2}(z_{k,i,j+1}^{\mathrm{ag}}-2z_{k,i,j}^{\mathrm{ag}}+z_{k,i,j-1}^{\mathrm{ag}})\\&+\alpha_2\frac{\Delta t}{2\Delta s}(z_{k,i,j+1}^{\mathrm{ag}}-z_{k,i,j-1}^{\mathrm{ag}})+\zeta_2 z_{k,i,j}^{\mathrm{ag}},\end{aligned} \tag{28}$$

Authorized licensed use limited to: Texas Tech University. Downloaded on March 19,2025 at 18:54:39 UTC from IEEE Xplore. Restrictions apply.

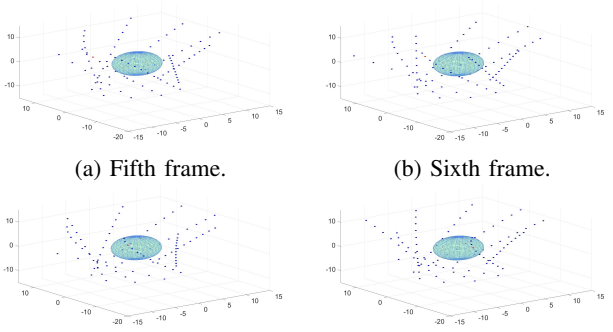

(a) Fifth frame. (b) Sixth frame.

(c) Seventh frame. (d) Eighth frame.

Fig. 8: Rotation of agents around targets with a secondary formation.

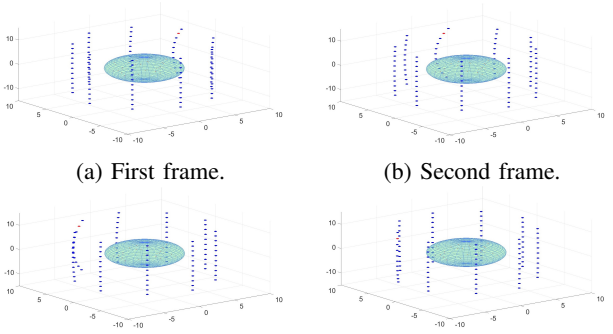

(a) First frame. (b) Second frame.

(c) Third frame. (d) Fourth frame.

Fig. 7: Rotation of agents around targets with a cylindrical formation.

has been used for interior points in the system and

$$u^{\text{ag}}_{k,i,1} = f_1(\theta_i), z^{\text{ag}}_{k,i,1} = f_2(\theta_i), \tag{29}$$

$$u^{\text{ag}}_{k,i,m} = g_1(\theta_i), z^{\text{ag}}_{k,i,m} = g_2(\theta_i), \tag{30}$$

$$u^{\text{ag}}_{k,n,j} = u^{\text{ag}}_{k,1,j}, z^{\text{ag}}_{k,n,j} = z^{\text{ag}}_{k,1,j}, \tag{31}$$

are the boundary points. Controllers are discretized accordingly.

B. Numerical example

Consider a group of $p = 20$ dynamic targets within a sphere centered at $\boldsymbol{w}^\star = [35, 0, 35]^T$ with a radius of $r^\star = 10$. We have $n = 10$, $m = 11$ in total 110 agents. The system parameters are set as $\alpha_1 = 0$, $\alpha_2 = 0$, $\zeta_1 = 1$, and $\zeta_2 = 1$ at first and after some time at we have change them to $\alpha_1 = 10 + 3j$, $\alpha_2 = 0$, $\zeta_1 = 80$, and $\zeta_2 = 1$ to shape a second formation around targets.

Each step has a unique desired formation or geometric center, summarized in Table I. Note that $k = 1.5$ and $\xi = 2$ in this section.

The boundary conditions of the system are as follows

$$f_1 = g_1 = kr^\star e^{j\theta}, f_2 = -10, g_2 = 10. \tag{32}$$

Agents start this step at their final positions from the previous step with $t_{\max} = 3$, as shown in Fig. 7a. Figures 7 and 8 display eight sub-figures of agent movements in step 4, showing rotations around targets and formation changes over time. A video of all step frames is available in [16].

V. Conclusion and Future Works

This paper introduced a novel rotational encirclement control for PDE-based multi-agent systems, focusing on multi-step in-domain control. After successful encirclement, agents faced challenges in maintaining it. In-domain control was used to address these issues, with stability analyzed via the Lyapunov technique. Simulations were performed to assess the methodology's effectiveness.

Future work will focus on relative coordinates, improving Step 1 by guiding agents towards targets, and developing methods for dynamic target spheres, including providing agents with estimators for the dynamic center and radius.

References

[1] C. Canuto, F. Fagnani, and P. Tilli, "A Eulerian approach to the analysis of rendez-vous algorithms," *IFAC Proceedings Volumes*, vol. 41, no. 2, pp. 9039–9044, 2008.

[2] P. Frihauf and M. Krstic, "Leader-enabled deployment onto planar curves: A PDE-based approach," *IEEE Transactions on Automatic Control*, vol. 56, no. 8, pp. 1791–1806, 2010.

[3] M. Hasanzadeh and S.-X. Tang, "Dynamic average consensus as distributed pde-based control for multi-agent systems," in *2024 European Control Conference (ECC)*. IEEE, 2024, pp. 828–833.

[4] G. Ferrari-Trecate, A. Buffa, and M. Gati, "Analysis of coordination in multi-agent systems through partial difference equations," *IEEE Transactions on Automatic Control*, vol. 51, no. 6, pp. 1058–1063, 2006.

[5] P. Barooah, P. G. Mehta, and J. P. Hespanha, "Mistuning-based control design to improve closed-loop stability margin of vehicular platoons," *IEEE Transactions on Automatic Control*, vol. 54, no. 9, pp. 2100–2113, 2009.

[6] J. Qi, R. Vazquez, and M. Krstic, "Multi-agent deployment in 3-D via PDE control," *IEEE Transactions on Automatic Control*, vol. 60, no. 4, pp. 891–906, 2014.

[7] M. Tavakoli, G. Cabrita, R. Faria, L. Marques, and A. T. de Almeida, "Cooperative multi-agent mapping of three-dimensional structures for pipeline inspection applications," *The International Journal of Robotics Research*, vol. 31, no. 12, pp. 1489–1503, 2012.

[8] T. Meurer and M. Krstic, "Finite-time multi-agent deployment: A nonlinear PDE motion planning approach," *Automatica*, vol. 47, no. 11, pp. 2534–2542, 2011.

[9] J. Zhang, R. Vazquez, J. Qi, and M. Krstic, "Multi-agent deployment in 3-D via reaction–diffusion system with radially-varying reaction," *Automatica*, vol. 161, p. 111491, 2024.

[10] J. Qi, S.-X. Tang, and C. Wang, "Parabolic PDE-based multi-agent formation control on a cylindrical surface," *International Journal of Control*, vol. 92, no. 1, pp. 77–99, 2019.

[11] M. Hasanzadeh, M. Baradarannia, and F. Hashemzadeh, "Distributed fixed-time rotating encirclement control of linear multi-agent systems with moving targets," *Journal of the Franklin Institute*, p. 106970, 2024.

[12] I. Shevchenko, "Guaranteed strategies for escaping encirclement," *Automation and Remote Control*, vol. 78, pp. 1892–1908, 2017.

[13] X. Wang, Y. Shi, R. Li, and Y. Bao, "Target-enclosing for multi-agent systems at same height," in *Proceedings of 2018 Chinese Intelligent Systems Conference: Volume II*. Springer, 2019, pp. 507–518.

[14] M. Hasanzadeh and S.-X. Tang, "Distributed dynamic encirclement control for first-order multi-agent systems with communication delay," in *2024 American Control Conference (ACC)*. IEEE, 2024, pp. 1000–1005.

[15] ——, "Encirclement control for PDE-based leader-follower multi-agent systems with targets in a sphere: Part 1 – target enclosing," *IEEE Conference on Decision and Control*, 2024.

[16] ——, "Encircling.mp4," 2024, https://www.dropbox.com/scl/fi/mj7syiujbowotg8cupzcu/Encircling.mp4?rlkey=k8ovwr55sld6lw2u3fvx4endv&dl=0.

Authorized licensed use limited to: Texas Tech University. Downloaded on March 19,2025 at 18:54:39 UTC from IEEE Xplore. Restrictions apply.